IOPscience

HOME | SEARCH | PACS & MSC | JOURNALS | ABOUT | CONTACT US

High-resolution hydrogen profiling in AlGaN/GaN heterostructures grown by different epitaxial methods

This article has been downloaded from IOPscience. Please scroll down to see the full text article.

2009 J. Phys. D: Appl. Phys. 42 055406

(http://iopscience.iop.org/0022-3727/42/5/055406)

The Table of Contents and more related content is available

Download details:
IP Address: 129.8.242.67
The article was downloaded on 12/09/2009 at 11:21

Please note that terms and conditions apply.

IOP PUBLISHING JOURNAL OF PHYSICS D: APPLIED PHYSICS

J. Phys. D: Appl. Phys. **42** (2009) 055406 (5pp) doi:10.1088/0022-3727/42/5/055406

High-resolution hydrogen profiling in AlGaN/GaN heterostructures grown by different epitaxial methods

F González-Posada Flores[1,6], A Redondo-Cubero[1,2], R Gago[2,3], A Bengoechea[1], A Jiménez[4], D Grambole[5], A F Braña[1,7] and E Muñoz[1]

[1] Instituto de Sistemas Optoelectrónicos y Microtecnología (ISOM) and Dpto. Ingeniería Electrónica (DIE), ETSI de Telecomunicación, Universidad Politécnica de Madrid, E-28040 Madrid, Spain
[2] Centro de Micro-Análisis de Materiales, Universidad Autónoma de Madrid, E-28049 Madrid, Spain
[3] Instituto de Ciencia de Materiales de Madrid, Consejo Superior de Investigaciones Científicas, E-28049 Madrid, Spain
[4] Dpto. Electrónica, Escuela Politécnica Superior, Universidad de Alcalá, E-28805 Alcalá de Henares, Madrid, Spain
[5] Institute of Ion Beam Physics and Materials Research, Forschungszentrum Dresden-Rossendorf, PF 51019, D-01314 Dresden, Germany

E-mail: fposada@die.upm.es

Received 18 December 2008, in final form 19 January 2009
Published 19 February 2009
Online at stacks.iop.org/JPhysD/42/055406

Abstract

Hydrogen (H) incorporation into AlGaN/GaN heterostructures used in high electron mobility transistors, grown by different methods, is studied by high-resolution depth profiling. Samples grown on sapphire and Si(1 1 1) substrates by molecular-beam epitaxy and metal–organic vapour phase epitaxy; involving H-free and H-containing precursors, were analysed to evaluate the eventual incorporation of H into the wafer. The amount of H was measured by means of nuclear reaction analysis (NRA) using the $^{1}H(^{15}N,\alpha\gamma)^{12}C$ reaction up to a depth of ∼110 nm into the heterostructures. Interestingly, the H profiles are similar in all the samples analysed, with an increasing H content towards the surface and a negligible H incorporation into the GaN layer (0.24 ± 0.08 at%) or at the AlGaN/GaN interface. Therefore, NRA shows that H uptake is not related to the growth process or technique employed and that H contamination may be due to external sources after growth. The eventual correlation between topographical defects on the AlGaN surface and the H concentration are also discussed.

(Some figures in this article are in colour only in the electronic version)

1. Introduction

The lifetime and performance of microelectronic and optoelectronic devices in III–V semiconductors, especially those based on AlGaN/GaN heterostructures, is considerably affected by the presence of impurities, trapping centres and point and linear defects. For instance, hydrogen (H) passivation of acceptors was a serious difficulty in obtaining p-type GaN. Therefore, H contamination is a crucial point for the development of reliable devices. Moreover, addressing the role and incorporation pathways of H in wide band gap semiconductors is of great interest from both the fundamental and technological points of view and it is expected to have an increasing importance in the future [1–6].

The impact of the H impurities in semiconductor physics is complex since several effects can be induced simultaneously, such as dangling bonds termination, passivation or compensation of both shallow and deep defects and the generation of extended defects [7]. On the other hand, the presence of H can be used to reveal defects in the atomic structure by 'decorating' them, i.e. H atoms become bonded to defect

[6] Author to whom any correspondence should be addressed.
[7] Present address: BP Solar, Polígono Industrial Zona Oeste S/N, 28760 Tres Cantos.

 © 2009 IOP Publishing Ltd Printed in the UK

Table 1. Selected structural, surface and electrical characterization results and $[H_0]$ and $[H_B]$ measured by NRA at ∼5 and 110 nm, respectively (mean values and standard deviation are presented).

Sample	Growth method	Precursor	Substrate	$FWHM_{GaN}$ (arcmin)	[Al] (%)	DD (10^9 cm^{-2})	SR (nm)	$[H_0]$ (at%)	$[H_B]$ (at%)
A	MOPVE	NH_3	Al_2O_3	7.5 ± 0.6	31 ± 2	9 ± 2	0.9 ± 0.3	0.9 ± 0.1	0.2 ± 0.1
B	MBE	NH_3	Si(1 1 1)	17 ± 2	35 ± 3	1.9 ± 0.2	1.7 ± 0.7	0.83 ± 0.07	0.23 ± 0.06
C	MBE	N_2	Si(1 1 1)	15.0 ± 0.8	29 ± 7	5 ± 2	5 ± 1	6 ± 3	0.31 ± 0.05
D	MBE	N_2	Al_2O_3	5 ± 1	26 ± 6	0.3 ± 0.2[a]	0.6 ± 0.2	2 ± 1	0.22 ± 0.08

[a] Screw dislocation density value.

lattice nearest neighbours [5]. GaN-based materials grown by molecular-beam epitaxy (MBE) and metal–organic vapour phase epitaxy (MOVPE) can present a very high H concentration ([H] $\sim 10^{20}$ cm^{-3}) due to the residual pressure during deposition or direct incorporation from the growth precursors [5]. Although other growth precursors have been studied as a route to achieve H-free GaN [9], most industrial semiconductor manufacturing is done in a H contaminated environment, where atomic H seems to be unintentionally incorporated to III-nitrides during processing steps [10], for instance in high electron mobility transistors (HEMTs) and UV light emitting devices.

AlGaN/GaN heterostructures are widely used in device design, and knowledge of the potential presence and effects of H is of great importance. So far, studies that explicitly address point defects and their interaction with H in AlGaN compounds are rare. Despite the lack of detailed information about AlGaN native defects, their properties can be obtained by interpolating the data between AlN and GaN, as a first approximation [11]. Moreover, H incorporation and diffusion in n-type, intrinsic and p-type GaN have been studied [11, 12], but to our knowledge, no study in AlGaN/GaN heterostructures has been reported. In addition, the majority of the studies found in the literature related to H incorporation use deuterium (D) instead of H to enhance the sensitivity detection by secondary ion mass spectrometry (SIMS) [10]. Elastic recoil detection analysis has also been used to verify a D monolayer presence related to an AlGaN/GaN organic gate gas sensor used in gas detection [13]. Nuclear reaction analysis (NRA) in p-type Mg doped GaN has also been carried out and resulted in good agreement with D SIMS profiling [12].

This work focuses on the presence of H in strained AlGaN/GaN heterostructures and its effect on the two-dimensional electron gas (2DEG) properties. We present [H] depth profiling analysis with high resolution in AlGaN/GaN heterostructure layers up to a depth of ∼110 nm. Samples were grown on two different substrates, sapphire and Si(1 1 1), using NH_3 and N_2-plasma as growth precursors. NRA was used for H content determination by means of the $^1H(^{15}N,\alpha\gamma)^{12}C$ reaction. The analysis is not sensitive to the ionization state of the H atoms and, thus, all electrically active complexes (H^+ and H^-) and neutral complex are measured. The results show that H uptake is not related to the growth process or technique employed and that H contamination is related to post-deposition air exposure.

2. Material and experimental

In our study, AlGaN/GaN heterostructures were grown by MOVPE (samples type A) and MBE (samples type B–D) methods. The conditions for each type of samples are grouped in table 1. In the case of MBE, both NH_3 (sample B) and N_2-plasma (samples C and D) gas precursors were used. Samples were grown on sapphire and Si(1 1 1) substrates. The thickness of the AlGaN layer was 20–25 nm in all the cases, grown onto a GaN buffer with different nucleation layers. The samples grown with a NH_3-MBE also have a 2 nm GaN cap. Samples of 1×1 cm^2 size were analysed after organic cleaning based on acetone (heated for two minutes) and methanol ultrasonic bath for 2 min.

The aluminium content ([Al]) of the AlGaN barrier, the relaxation parameter and the rocking curve full-width at half maximum (FWHM) were obtained by x-ray diffraction (XRD) in a 3D Bede Scientific Diffractometer. Sheet resistance (R_s) was measured using a Leighton system and mobility (μ) was determined by Van der Pau measurements in an Accent HL5500 Hall system. 2DEG density (n_s) was determined by a Hg-CV profiler. Surface roughness (SR) was extracted using a Nanoscope III Veeco atomic force microscope (AFM).

The H content was measured by high depth resolution by means of NRA using the $^1H(^{15}N,\alpha\gamma)^{12}C$ reaction [14]. In this case, 4.43 MeV γ-rays are produced resonantly for a projectile energy of 6.385 MeV. The emitted radiation is then detected with a 100 mm diameter and 100 mm long BGO detector placed about 20 mm behind the sample. Depth profiling was obtained by sweeping the energy of the impinging ^{15}N ions around the resonance value, while the H content was determined by the total number of characteristic γ-rays [15]. The detection limit under these conditions is 0.02 at%. Considering the stopping power for crystalline GaN obtained by the SRIM code [16] and the energy width of the resonance (∼12 keV), the depth resolution of this method is less than 4 nm. The details of the experimental setup can be found elsewhere [17].

3. Experimental results

As shown in table 1, sample D presents the narrowest FWHM and thus the highest crystalline quality [18] of all samples, followed closely by sample A. The [Al] derived from XRD ranges from 20 up to 40%. AFM images shown in figure 1 reveal the presence of morphological defects (pits and nanocracks) and dislocations (edge and screw type). Dislocation density (DD) was measured in 1×1 and 2×2 μm^2 images. In

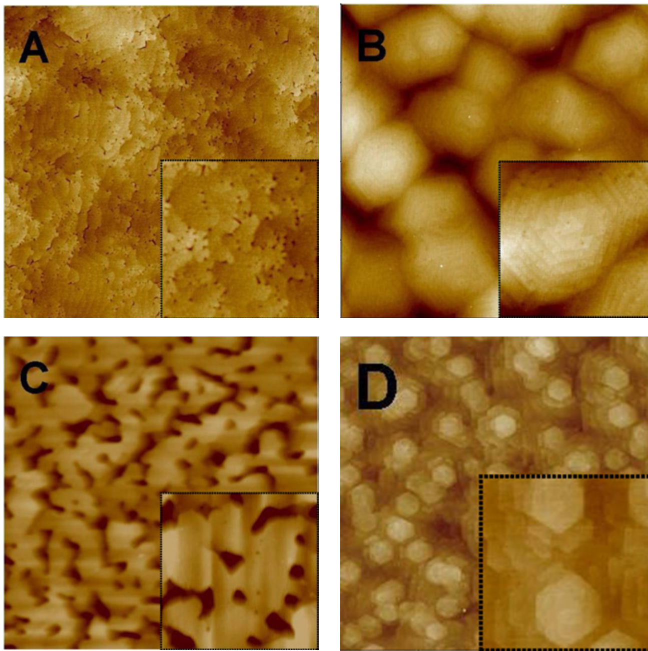

Figure 1. AFM 4 × 4 μm^2 images (inset image size is 1 × 1 μm^2) of the AlGaN/GaN heterostructures. The label of each figure corresponds to the sample reference. The image (inset) height scale limit is 12.5 (12.5) nm, 20 (12) nm, 25 (20) nm and 8 (8.5) nm for samples A, B, C and D respectively.

D and B sample surfaces, clear differences between screw and edge dislocation were found, being the screw DD (3 ± 2) and $(1.8 \pm 0.3) \times 10^8$ cm^{-2}, respectively. Sample A has the highest DD, $(9 \pm 2) \times 10^9$ cm^{-2}, where dislocations have mostly a nanometric size (1–10 nm) and enlarged shape occasionally. Surface DD estimated for the C wafer is in the same range as in A and B samples, but defect sizes are higher. SR was analysed in 0.5 × 0.5–4 × 4 μm^2 images. In C sample SR is clearly higher due to pits and cracks on the surface, with 50–150 nm lateral size and 17 ± 5 nm deep. Additionally, the electrical characteristics of some samples show typical values of $\mu \sim 770 \pm 40$ cm^2 V^{-1} s^{-1}, $R_s \sim 520 \pm 30\Omega/\square$ and $n_s \sim (7 \pm 3) \times 10^{12}$ cm^{-2}. These values are in the usual range for standard AlGaN/GaN HEMT technology.

Figure 2 shows the obtained high-resolution H profile, starting from the sample surface up to ~110 nm into the AlGaN/GaN heterostructures for the different samples. Neither the growth method (NH_3-MBE, N_2-plasma MBE or MOVPE) nor the substrate (Si(1 1 1) or sapphire) seems to affect the H detected in the AlGaN/GaN heterostructures. This result indicates that no significant H incorporation is produced during the growth process. Moreover, in-depth H profiles are decreasing and very close to an exponential behaviour, which can be described by interdiffusion mechanisms due to trapping effects [19]. Therefore, we can conclude that H profiles are related to external sources after deposition.

Table 1 summarizes the experimental [H] at the near surface ($[H_0]$) and at the maximum analysed depth ($[H_B]$). The value of $[H_0]$ for the MOVPE and NH_3-MBE samples is close to 1%, while higher values were found for N_2-plasma MBE growth. These values are similar to SIMS results

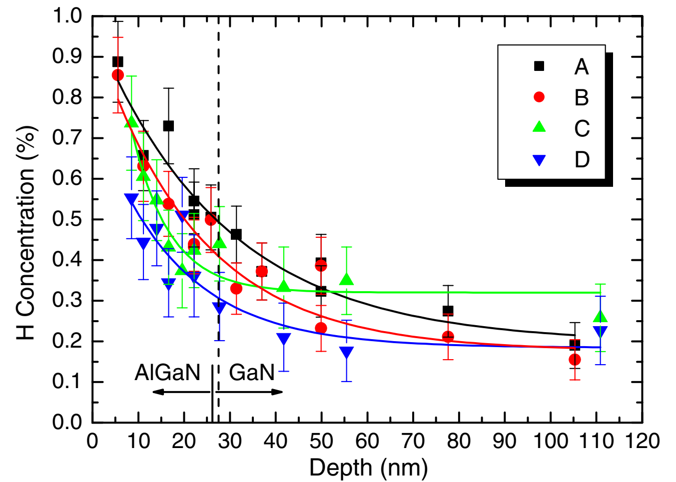

Figure 2. NRA of [H] profile for NH_3 (samples A and B) and N_2-plasma (samples D and C) growth precursors. Solid line (colour on-line) is the simulation of the H profile. NRA instrumental depth error is ~4 nm and AlGaN/GaN separation in x-scale is figurative.

published by Pearton *et al* [20]. H content in the AlGaN/GaN interface is close to 0.5–0.4% (see figure 2), but a different exponential decrement could be pointed out between NH_3 and N_2-plasma assisted growths. Finally, mean $[H_B]$ detected was 0.24 ± 0.09 at% for the seventeen samples included in this study.

In more established semiconductors such as Si and GaAs, H behaviour is well understood [19]. However, the behaviour of H in n- and p-type GaN is predicted to be different from more traditional semiconductors and even between the two GaN types mentioned above [11]. The build-up of H in the [H] profiles (Δ[H]) is usually related to strained regions in GaN-based structures, such as interfaces and bulk and/or surface defects [10, 20]. In our study, AlGaN/GaN wafers were grown pseudomorphically, where the AlGaN layer tends to be completely strained on the GaN layer, as verified by XRD (not shown here). Contrary to what would be expected, figure 2 shows no Δ[H] at the AlGaN/GaN interface and corroborates the low H incorporation during growth. In addition, the presence of charge in the 2DEG could be considered as another preferential site but, as seen in figure 2, no Δ[H] is measured. This result was verified by measuring the H-NRA profile several times in the 25–50 nm region for samples A and B. In conclusion, the H profile is sensible to neither the AlGaN/GaN interface nor the 2DEG presence in the heterostructures.

4. Discussion

In order to analyse quantitatively the experimental [H] profiles, simulations considering different incorporation mechanisms were carried out. For this, we considered our sample as a semi-infinite medium and keeping a constant H concentration at the surface, where the Fick's equation solution for diffusion is the well-known complementary error-function, erfc(Z) [19]. Levenberg–Marquardt algorithm was used to reduce residual parameters and obtain a better accuracy [21]. However, the simulations did not fit accurately with the experimental data.

Table 2. H-profile simulation parameters (mean values and standard deviation are presented).

Sample	R^2	H_B (at%)	$\bar{x}$ (nm)	$[H_0]$ (at%)
A	0.92 ± 0.02	0.22 ± 0.08	29 ± 6	1.0 ± 0.2
B	0.84 ± 0.09	0.26 ± 0.07	24 ± 4	0.93 ± 0.07
C	0.8 ± 0.2	0.35 ± 0.03	7 ± 3	4 ± 3
D	0.82	0.18 ± 0.06	18 ± 9	0.8 ± 0.2

Consequently, the trapping effect has to be considered into the model. When this is taken into account, the solution of the diffusion equation for the steady-state regime gives an exponential function for H composition, $[H] = [H_0] \times \exp(-\alpha Z)$, where the αZ parameter is related to the capture radius for the H reaction as impurity [19]. Nevertheless, the simulation accuracy was still very poor in this case. Consequently, no longer can the present [H] be considered as a doping level diffused into the AlGaN/GaN heterostructures and this apparent diffusivity falls off because of the closer experimental data profile to a H trapping exponential profile. Profiles simulations were done taking into account a constant background $[H_B]$ as a new parameter for the simulation, as follows: $[H] = H_B + H_S \times \exp(-x/\bar{x})$. Here the H_B parameter is related to the background [H], the H_S parameter is related to $[H_0]$ by $H_S = [H_0] - H_B$ and $\bar{x}$ is the mean diffusion distance. For simple effects as trapping impurity, diffusion equations do not hold, and usually one chooses $\bar{x}$ to be the distance at which the profile falls to one-half the maximum concentration in the profile [19].

Table 2 summarizes the parameters obtained from the proposed constant background simulation. The H_B values and $[H_0]$ calculated, at least to a 110 nm depth, are similar to the experimental concentrations shown in table 1. The value $\bar{x}$ extracted from the fitting is 29 ± 6 nm and 24 ± 4 nm for the samples grown by MOVPE and MBE, respectively. Since in the samples grown by N_2-plasma MBE, $[H_0]$ was strongly higher, the simulations do not yield consistent results. However, $\bar{x}$ is estimated to be 7 ± 3 and 18 ± 9 nm for samples C and D, respectively. Thus, a significant decrease in $\bar{x}$ is happening for these samples, as can be seen from the exponential decay in figure 1.

Regarding $[H_B]$, similar concentration values were detected by NRA for all the samples (see table 1). However, comparing the FWHM values of the XRD Bragg reflections for C and D samples (see table 1) and taking into account that they were grown by the same N_2-plasma MBE technique, we can assume that the slight difference in $[H_B]$ may be due to the strong enhancement of H in-diffusion by the presence of the high defect density in the heterostructure. This result supports the suggestions given in [3].

From figure 1, the AlGaN surface dislocation/defect counting reveals a DD for the C samples in the same range ($\sim 10^9$ cm^{-2}) as compared with the A, B and D samples. However, figure 1 shows that the AFM surface defects/dislocations in sample C have a bigger size and SR increases up to 5 ± 1 nm, where $[H_0]$ measured was 6 ± 3 at%. These results suggest that SR, DD and defect sizes are related somehow to the $[H_0]$ difference, in agreement with Mimila-Arroyo *et al* [3], where $[H_0]$ differences were related to plasma-induced defects compared with defect free surfaces in nonintentional doped GaN. Moreover, H diffusion pathways along threading dislocations have been speculated [3], thus dislocation/defect density size distribution may be affecting the [H] profile in agreement with the slight differences between $[H_B]$ in the different types of samples (see table 1).

From table 1, $[H_B]$ and $[H_0]$ are high enough to take seriously the hypothesis made by Van de Walle and Neugebauer [22], who indicated that H atoms are probably part of the basic building blocks of the GaN and AlGaN atomic structure and play changes in the surface reconstructions under realistic growth conditions and in post-growth processing.

Hence, it is possible that through external sources such as air exposure, sample surface cleaning (organics and acids) and/or further processing (by reactive ion etching or chemical vapour deposition methods); both H^+ and H^- are formed at the surface and diffuse inside the sample. Theoretical calculations on GaN [7, 8], and also measurements, show that H^+ diffuses dominantly into n-type GaN layers [23], and H^- will do the same into p-type GaN [24]. However, no easy assumption could be made of which ionization state, H^+ or H^-, will diffuse into the AlGaN/GaN heterostructures, as no effect was detected at the 2DEG or the AlGaN/GaN interface.

Typically, defect formation energies are lower at the surface than in the bulk, resulting in high defect concentrations at the surface [11]. From the AFM images of figure 1, the surface of the C sample shows the presence of bigger and deeper morphological defects as compared with the A and B samples. Moreover, SR for the C sample, 5 ± 1 nm, is almost three times higher than in the B sample, SR 1.7 ± 0.7 nm, and the latter is almost twice as A sample, SR 0.9 ± 0.3 nm. Similarly to the SR difference, $[H_0]$ seems to increase (see table 1). For the C sample compared with the A and B samples, the $[H_0]$ difference is 5 at%, approximately. In contrast, the difference in $[H_0]$ for the A and B samples is smaller (0.9 ± 0.1 at% and 0.83 ± 0.07 at%, respectively). Summarizing, the defects for sample C are rather bigger in size to screw and edge dislocations detected in the B sample. Usually, a higher SR involves a bigger surface exposition to the air, as shown in figure 1 for sample C, and a higher H incorporation was detected at the surface of sample C compared with the B one; thus, we can conclude that a high surface defect density, i.e. higher SR, could be related to a higher [H].

The solubility limit corresponds to the maximum concentration that an impurity can attain in a semiconductor, under conditions of thermodynamic equilibrium [11]. If NH_3 and N_2-plasma grown wafer sets are compared (see table 1), the mean solubility of H in the heterostructures analysed is limited, on average, to 0.24 ± 0.08 at%, which represents twice the residual pressure found in a growth chamber [5, 16]. Over short length scales, it may still be possible the diffusion of the first few atomic layers beneath the surface for limited equilibration [11]. In consequence, we can assume that H incorporation could be *ex situ* as a contamination through the surface which is able to diffuse, as a minimum, deep to

∼110 nm in the heterostructures, independently of the growth technique and the substrate used.

Last but not least, AlGaN/GaN HEMT technology is always struggling with passivation, which is normally attained with silicon nitride (SiN) overlayers. The complex SiN deposition mechanisms by chemical vapour deposition methods enables H to be incorporated in the passivant layer [25] and thus to be in contact with the AlGaN surface. A closer look should be taken of the H interdiffusion, once HEMT processing is finished, assuming a 24–29 nm mean diffusion distance mentioned above.

5. Conclusions

We have tried to answer a relevant question about the eventual presence of H in as-grown AlGaN/GaN heterostructures. By means of high-resolution depth profiling by NRA, a H maximum content of 0.24 ± 0.08 at% has been determined in a set of AlGaN/GaN heterostructures (up to a depth of ∼110 nm). It is remarkable that neither at the 2DEG nor at the AlGaN/GaN interface, were effects in relation to H accumulation detected. AlGaN [H] at the surface seems to be related to a higher defect density. Due to the high H background detected, *ex situ* post-growth H incorporation is postulated. To conclude, there is no influence of the epitaxial growth method (NH_3-MBE, NH_3-MOVPE and N_2-plasma MBE), nor the substrate (sapphire versus Si), on the [H] profiles determined in the AlGaN/GaN HEMT heterostructures characterized in this study.

Acknowledgments

The authors are indebted to Dr Mykola Vinnichenko for his assistance with the NRA measurements. This work has been carried out inside the KORRIGAN project (EU-FP6 contract No MOU 04/102.052/032). The experiments at AIM (FZD-Rossendorf) were supported by the EU 'Research Infrastructures Transnational Access' program under EC contract No 025646. The authors also thank IMS-NRC (Canada) for their assistance. This work was partially supported by a FPU research grant from the Spanish Ministry of Education. QinetiQ and Picogiga, partners of the KORRIGAN project, are specially acknowledged for supplying heterostrucutres grown by MOPVE on sapphire and by NH_3-MBE on Si(1 1 1).

References

[1] Hasegawa H and Akazawa M 2008 *Appl. Surf. Sci.* **254** 3653–66
[2] Naono T, Fujiokaa H, Okabayashi J, Oshima M and Miki H 2006 *Appl. Phys. Lett.* **88** 152114
[3] Mimila-Arroyo J, Barbé M, Jomard F, Chevallier J, di Forte-Poisson M A, Delage S L and Dua C 2007 *Appl. Phys. Lett.* **90** 072107
[4] Zhang S B, Janotti A, Wei S H and Van de Walle C G 2004 *IEE Proc. Optoelectron.* **151** 369–78
[5] Chevallier J and Pajot B 2002 *Solid State Phenom.* **85–86** 203–84
[6] Polyakov A Y, Shin M, Freitas J A, Skowronski M, Greve D W and Wilson R G 1996 *J. Appl. Phys.* **80** 6439–46
[7] Neugebauer J and Van del Walle C G 1995 *Phys. Rev. Lett.* **75** 4452–5
[8] Neugebauer J and Van del Walle C G 1996 *Appl. Phys. Lett.* **68** 1829–31
[9] McMurran J, Todd M, Kouvetakis J and Smith D J 1996 *Appl. Phys. Lett.* **69** 203–5
[10] Pearton S J, Abernathy C R, Vartuli C B, Mackenzie J D, Shul R J, Wilson R G and Zavada J M 1995 *Electron. Lett.* **31** 836–7
[11] Van de Walle C G and Neugebauer J 2004 *J. Appl. Phys.* **95** 3851–79
[12] Myers S M, Wright A F, Petersen G A, Seager C H, Wampler W R, Crawford M H and Han J 2001 *J. Appl. Phys.* **89** 3195–202
[13] Winzer A T, Goldhahn R, Gobsch G, Dadgar A, Krost A, Weidemann O, Stutzmann M and Eickhoff M 2006 *Appl. Phys. Lett.* **88** 024101
[14] Landford W A, Trutvetter H P, Ziegler J F and Keller J 1976 *Appl. Phys. Lett.* **28** 566–9
[15] Rudolph W, Grambole D, Grötzschel R, Heiser C, Herrmann F, Knothe P and Neelmeijer C 1988 *Nucl. Instrum. Methods* B **33** 503–11
[16] Ziegler J F, Biersack J P and Littmark U 1985 *The Stopping and Ranges of Ions in Solids* (Oxford: Pergamon)
[17] Rudolph W, Bauer C, Brankoff K, Grambole D, Grötzschel R, Heiser C and Herrmann F 1986 *Nucl. Instrum. Methods* B **15** 508–11
[18] Bauer G and Richter W 1996 *Optical Characterization of Epitaxial Semiconductor Layers* (Berlin: Springer
[19] Pearton S J, Corbert J W and Stavola M 1992 *Hydrogen in Crystalline Semiconductors (Springer Series in Material Science)* (Berlin: Springer)
[20] Pearton S J, Cho H, Ren F, Chyi J I, Han J and Wilson R G 2000 *MRS Internet J. Nitride Semicond. Res.* **5S1** F99 W10.6
[21] Marquardt D W 1963 *SIAM J. Appl. Math.* **11** 431–41
[22] Van de Walle C G and Neugebauer J 2002 *Phys. Rev. Lett.* **88** 066103
[23] Hierro A, Ringela S A, Hansen M, Speck J S, Mishra U K and DenBaars S P 2000 *Appl. Phys. Lett.* **77** 1499–501
[24] Götz W, Johnson N M, Bour D P, McCluskey M D and Halle E E 1996 *Appl. Phys. Lett.* **69** 3724–26
[25] Redondo-Cubero A, Gago R, Romero M F, Jiménez A, González-Posada F, Braña A F and Muñoz E 2008 *Phys. Status Solidi* c **5** 518–21